

Article

Colorimetric Gas Detection Using Molecular Devices and an RGB Sensor

Javier Roales ^{*}, Francisco G. Moscoso , Alejandro P. Vargas, Tânia Lopes-Costa and José M. Pedrosa ^{*}

Departamento de Sistemas Físicos, Químicos y Naturales, Universidad Pablo de Olavide, Ctra. Utrera Km. 1, 41013 Sevilla, Spain

^{*} Correspondence: jroabat@upo.es (J.R.); jmpedpoy@upo.es (J.M.P.)

Abstract: Spectrophotometry and colorimetry are among the most-used techniques for chemical and biological analyses, but the required equipment is often expensive and restricted to laboratory use. We present here a low-cost and portable color measuring device that can provide similar results to laboratory spectrophotometers in color measuring applications. Our prototype was based on an RGB color sensor interfaced to a Raspberry Pi and mounted on custom sample holders with a dual illumination source for reflectance or transmittance measurements. To evaluate its capabilities for the detection of gases, we used two already-tested colorimetric molecular devices: Harrison's reagent supported on porous TiO₂ films for the detection of phosgene, and mixed films of a porphyrinic metal-organic frameworks and polydimethylsiloxane for the detection of biogenic amines. The results showed that the prototype could accurately monitor the color change of the sensing devices when exposed to the analytes and that its versatility allowed for the measurement of samples with different characteristics. This inexpensive and portable prototype, able to run on a 5 V battery and work wirelessly, proved to be a valid alternative for color measuring when expensive spectrophotometers are not available, mobility is needed, or a full-spectral characterization is not necessary.

Keywords: spectroscopy; color sensor; gas sensing; low-cost spectrophotometer



Citation: Roales, J.; Moscoso, F.G.; Vargas, A.P.; Lopes-Costa, T.; Pedrosa, J.M. Colorimetric Gas Detection Using Molecular Devices and an RGB Sensor. *Chemosensors* **2023**, *11*, 92. <https://doi.org/10.3390/chemosensors11020092>

Academic Editor: Simonetta Capone

Received: 24 December 2022

Revised: 19 January 2023

Accepted: 25 January 2023

Published: 27 January 2023



Copyright: © 2023 by the authors. Licensee MDPI, Basel, Switzerland. This article is an open access article distributed under the terms and conditions of the Creative Commons Attribution (CC BY) license (<https://creativecommons.org/licenses/by/4.0/>).

1. Introduction

Absorbance spectroscopy is one of the most common analytical techniques used for chemical and biological analyses. The high number of analyses that can be performed through this technique and its inexpensive cost per sample enables its use for routine analysis in laboratories across the world. However, the required instrumentation (i.e., spectrophotometers) have prices starting from around EUR 1000 (typically compact devices with a linear CCD sensor capable of recording the full spectrum at once) and can go up to EUR 60,000 (usually laboratory devices with a bigger footprint, more sophisticated lenses, and a mechanical monochromator to select the wavelength of the light source), depending on specifications and user requirements, which limits their use in developing countries, educational purposes, or low-budget research. Moreover, advanced spectrophotometers require trained personnel to operate and maintain the equipment, and an appropriate infrastructure in terms of stable electrical power is always necessary. In addition to this, although some analyses require a precise and full-spectral characterization of the sample, in many cases only a single wavelength or a simplified colorimetric approach is needed, such as when monitoring reactions with a clear color change (e.g., colorimetric indicators). In this scenario, a simple, low-cost device that can provide similar results to conventional spectrophotometers would be useful in cases when (i) a regular spectrophotometer is not available and cannot be afforded and/or (ii) a full-spectral characterization is not necessary.

Several approaches have been made to develop low-cost colorimetric detectors. One of them typically uses light-emitting diodes (LEDs) to illuminate the sample with a colored light from one side while a photodetector (photodiode or photoresistor) collects the resulting light from the other side of the sample [1–7]. Examples of applications based on this

kind of device include the detection of fluoride [8], chlorine [9], and mercury [10] in water samples, hemoglobin [11,12] in blood, or the measurement of seawater pH [13]. Despite the utility of these low-cost photometers for certain applications, they are restricted to the wavelengths emitted by the LED. Possible workarounds to tackle this limitation, such as implementing an array of differently colored LEDs and photodetectors, would result in more complex and expensive devices.

Another approach consists of the use of broadband light, which allows for more versatile measurements, usually comprising the visible region of the UV–vis spectrum. To conduct this, researchers have used white LEDs [14], flashlight bulbs [15], flatbed scanners [14,16], and digital displays such as smartphones [14,17] or computer screens [18]. When using broadband light, a diffraction grating and some moving parts are necessary if the photodetector is a photodiode or photoresistor so that the operator can select the incident wavelength. Examples of this are the LEGO spectrophotometer by Knagge et al. [15] or the low-cost spectrophotometer by Albert et al. [4]. Such setups, with educational purposes, provide teachers and students with useful tools to understand and experiment with spectrophotometric measurements but are not versatile enough to compete with laboratory-grade spectrophotometers. More sophisticated devices rely on linear CCD sensors, such as those installed in flatbed scanners, or CCD/CMOS image sensors, which can be found in smartphones and digital cameras. Either of these systems is composed of a large number of pixels, which makes them able to collect light at several wavelengths simultaneously. A diffraction grating may still be necessary to decompose white light into the colors of the visible spectrum depending on the specific setup and user requirements, but no moving parts are needed, and a complete spectrum can be recorded at once. For example, Christodouleas et al. [14] explored the abilities of a flatbed scanner and a smartphone-camera-based photometer effectively using these devices as RGB sensors and obtaining the RGB-resolved absorbances of the samples. Another example is the spectrophone developed by de Oliveira et al. [19], a portable smartphone-based spectrophotometer that uses a DVD slice as the diffraction grating and a smartphone as the imaging device and processing unit to obtain RGB-based spectra through an ad hoc algorithm.

These and other similar approaches take advantage of ubiquitous electronic devices such as smartphones, digital cameras or scanners, but have two main drawbacks. First, some of these devices, such as digital cameras or smartphones, can be expensive and, if they must be bought specifically for sensing purposes, they cannot be considered low cost. Second, in some cases the measurement involves the post-processing of the image taken by the device. Although this can be achieved without specialized software, it has to be conducted after the measurements are conducted and prevents the visualization of the data in real-time, which may be crucial in certain applications (e.g., toxic gas detection).

Here, we propose an RGB color sensor (Adafruit TCS34725) as a candidate for the color measurement of chemical processes where a color change takes place. This and other similar sensors have been used by other authors to measure microalgae concentrations in photo-bioreactors [20], to monitor plant leaf color as an indicator of plant status [21], or to measure olive oil [22], wine [23], or banana [24] color for quality control purposes. Our RGB color sensor, whilst inexpensive, was designed to accurately measure the color of a sample and provide the red (R), green (G), and blue (B) coordinates in the RGB color space. Given its small dimensions and low energy consumption, a portable setup of the device is possible. In this work, we will evaluate the real capabilities of a prototype based on this sensor as compared to laboratory-grade spectrophotometers. We will also evaluate whether the LED included in the sensor board (reflectance mode) or an external LED (transmittance mode) is more appropriate according to the sample to be measured. To achieve this, we will use the expertise of our research group in molecular sensing devices and adapt two of our most recent studies that dealt with colorimetric sensors whilst replacing the advanced laboratory spectrophotometers with this RGB sensor prototype. First, we will revisit our optical dosimeter for the detection of phosgene [25] based on Harrison's reagent embedded into nanocrystalline TiO₂ films. Second, we will explore new possibilities

for our mixed films made of a PCN-224 porphyrinic metal–organic framework (MOF) embedded in polydimethylsiloxane (PDMS) [26] and their capabilities for the detection of biogenic amines.

2. Materials and Methods

2.1. Chemicals

Phosgene (15% in toluene), diphenylamine, and 4-(dimethylamino)benzaldehyde were purchased from Sigma-Aldrich. Meso-tetra(4-carboxyphenyl)porphyrin (H₄TCPP) was obtained from Frontier Scientific. Other reagents and solvents were purchased as reagent-grade and used without further purification.

2.2. PCN-224 Synthesis

PCN-224 was synthesized following the method proposed by Feng et al. [27] with some modifications. First, 60 mg of ZrCl₄ and 800 mg of benzoic acid were ultrasonically dissolved in 2 mL of DMF in a Pyrex vial. Then, a solution of 20 mg of H₂TCPP in DMF was poured into the previous solution. Subsequently, the mixture was placed in an oven for 24 h at 120 °C. The product was collected in the form of a dark-purple powder after centrifugation at 6000 rpm and washed three times with fresh DMF and finally once with methanol. At the end of the procedure, the crystals were dried in air at room temperature.

2.3. Films Preparation

2.3.1. Phosgene Detection Films

We infiltrated Harrison's reagent (a 0.37 M equimolar mixture of diphenylamine and 4-((dimethylamino) benzaldehyde) into nanocrystalline TiO₂ films. These films were made by screen-printing two layers of transparent titania paste (18NR-T, Dyesol, Queanbeyan, Australia) onto glass substrates through a 90T mesh screen to form a transparent TiO₂ film with a 3 cm² active area. Before infiltration, the substrates with the screen-printed TiO₂ were sintered for 30 min at 500 °C. In a previous work [25], these films were characterized by scanning electron microscopy, finding that their average thickness was about 3 μm and that the matrix owned a high porosity with a homogeneous porous distribution that favored the interaction between the TiO₂ matrix and the sensing molecules, and later, with the analyte. The infiltration was performed by simple immersion of the TiO₂ films into a solution containing Harrison's reagent. Further details regarding this procedure can be found elsewhere [25].

2.3.2. Biogenic Amines Detection Films

We prepared flexible and self-adhesive films containing PCN-224 by mixing 20 mg of MOF powder with 5 g of dimethylvinyl-terminated PDMS (Sylgard 184, Dow Corning) and 0.5 g of dimethylhydrogen siloxane (curing agent). Afterwards, the mixture was spin-coated at 1000 rpm on a petri dish and placed in an oven overnight at 80 °C to end the polymerization. Self-adhesive PCN-224/PDMS films were obtained by cutting the required surface of the film with a scalpel and peeling it from the substrate. The resulting film could be easily transferred to another substrate—as a removable sticker—due to the self-adhesive nature of PDMS.

Prior to the sensing experiments, the porphyrin core of PCN-224 was protonated by exposing the PCN-224/PDMS films to trifluoroacetic acid (TFA) vapors. The protonation occurred immediately with a swift color change from reddish brown to green. Further details regarding this procedure can be found elsewhere [28].

2.4. Gas Sensing Experiments

Gaseous phosgene was obtained by flowing a stream of dry nitrogen through the headspace of a bottle that contained phosgene at 0 °C diluted in toluene at varying concentrations. The gaseous phosgene concentration was calculated according to its vapor pressure in the solution at the corresponding temperature and further diluted with a

second nitrogen stream until the desired concentration was obtained. The flow of both nitrogen streams was regulated by two Bronkhorst F-201FV mass flow controllers. After going through the gas chamber, the phosgene was neutralized by passing the gas outlet through a water filter. Further details on the gas exposure system and setup can be found elsewhere [25,29].

Biogenic amines were generated by storing small amounts of fish inside sealed transparent glass vials and leaving them at room temperature until natural decomposition occurred. Three species of fish were used: European anchovy (*Engraulis encrasicolus*), Atlantic salmon (*Salmo salar*), and Red mullet (*Mullus barbatus*). Before placing the fish samples in the vials, a 2 cm × 2 cm square of PDMS/PCN-224 film was adhered to the inner wall of each vial. This setup allowed for the direct measurement of the color of the film from the outside of the vial without opening it.

2.5. Prototype

2.5.1. RGB Sensor and Interfacing

The prototype was based on a TCS34725 RGB color sensor from Adafruit Industries (NYC, NY, USA). This sensor was chosen because of its low price (~10 €), reduced dimensions (2 cm × 2 cm), low power consumption, and versatility. Its low cost would allow for a multi-sensor arrangement if multiple simultaneous measurements were needed. It was interfaced through I2C connections to a Raspberry Pi 4B (Raspberry Pi, Cambridge, UK) that allowed us to easily modify the scripts and visualize the data in real time during the prototyping phase, although cheaper versions such as the Raspberry Pi Zero (~15 €) would work as well. Programming of the system was conducted using Python, the native coding language in the Raspberry Pi environment. We used the libraries provided by the sensor manufacturer and adapted them to our measurement requirements.

The versatility of the system, with its different possible setups, allowed us to measure the color of samples with varying characteristics and to visualize and/or save the data in different ways. Direct connection of peripherals such as a computer screen, a keyboard, and a mouse to the Raspberry Pi made possible the manipulation of the script in real time as needed, with the same capabilities and ease as a regular computer, although these devices would not be necessary for the standalone functioning of the prototype. For the measurement of toxic gases (i.e., phosgene), we remotely controlled the system via Wi-Fi and a smartphone, while the prototype was in an enclosed space in the presence of the analyte. Such a setup would also add to the portability of the system, eliminating the need for keyboard, mouse, or screen if the application required it. For the sake of illustration, a setup example is shown in Figure 1 with the TCS34725 RGB sensor and an external LED light mounted on a glass sample holder, a portable screen to visualize the script and monitor the sensor output, the Raspberry Pi, and a power source for the external LED light. In this example, the system was controlled wirelessly through a smartphone. All the components in this setup could work either plugged into AC power using their respective power adapter or using an external 5 V battery as a power source, such as those designed to power a smartphone. This was tested and worked flawlessly, which proved the portability of the prototype and its possibilities for the detection of gases where no electrical power can be found and/or when multiple sampling points are needed.

2.5.2. Light Sources

The illumination of the samples was conducted by either using the SMD white LED integrated in the TCS34725 board, meaning emitting the light perpendicularly from the plane of the sensor, such as when conducting a reflectance measurement using a spectrophotometer, or using an external white LED placed in front of the sensor at the opposite side of the sample with the light travelling through the sample and then reaching the sensor, such as when conducting a transmittance measurement in a spectrophotometer. This double setup allowed us to choose the best conditions for illumination according to the characteristics of the measured sample. Ambient light sources were blocked, and

no colored objects were present in the background or periphery of the sensor to avoid color contamination.

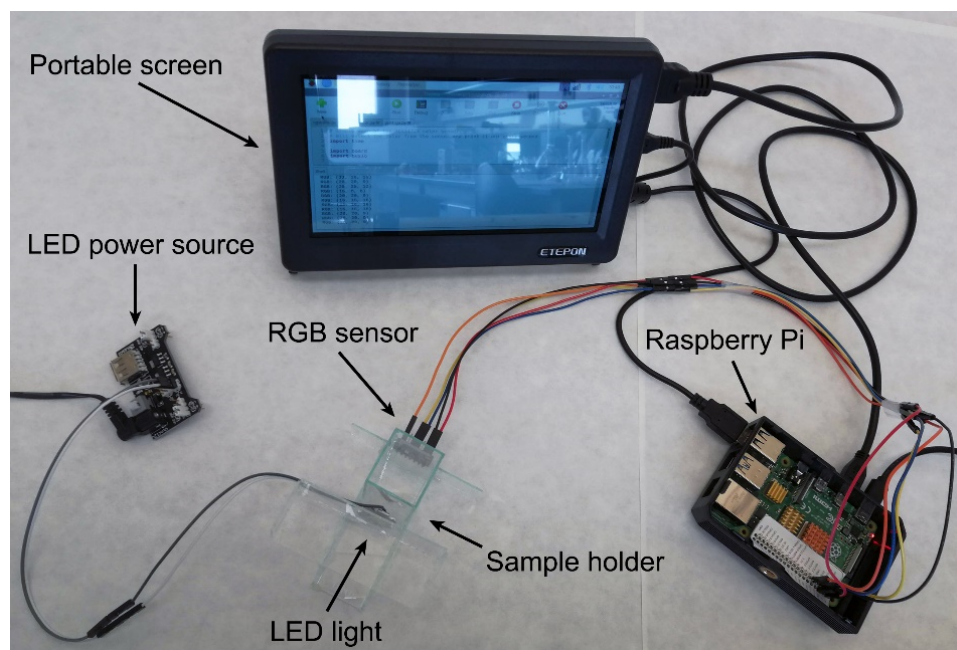


Figure 1. Example of setup: RGB sensor and external LED light mounted on a glass sample holder (bottom center), portable screen for script and output visualization (top center), Raspberry Pi (right), and external LED light power source (left).

2.5.3. Sample Holders

Two different sample holders were fabricated to allow for (i) open-air measurements, such as the detection of gaseous phosgene in the environment, and (ii) the analysis of gases in enclosed spaces, such as amines emitted from rotten fish in an enclosed space. The first was built using glass to withstand organic solvents and to permit direct external observation (Figure 2a). It consisted of a cuvette-like chamber and included the mounting for the RGB sensor and for the LED light, both on the outside and facing one another. The sensing film was installed on the inside of the chamber in front of the RGB sensor, covering it in its entirety. During the sensing experiments, the chamber was filled with the gaseous analyte of interest interacting with the sample but not with the electronic parts of the prototype.

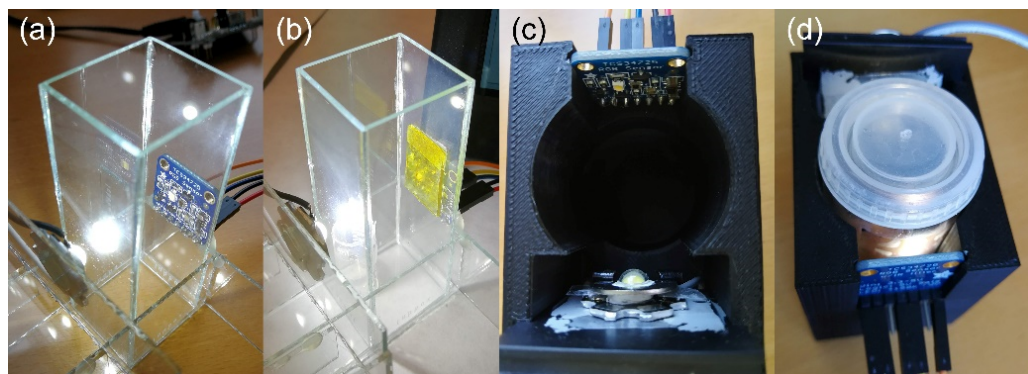


Figure 2. Measuring setup containing the sensor, light source, and sensing film. (a) Empty glass sample holder, (b) glass sample holder with a film for the detection of phosgene, (c) empty 3D-printed PLA sample holder, and (d) 3D-printed PLA sample holder with a glass vial containing a film for the detection of biogenic amines.

The second sample holder was custom-designed and 3D-printed using black polylactic acid (PLA) to block ambient light and to limit light reflection (Figure 2b). As in the other sample holder, it included mountings for the sensor and for the external LED light, which were facing one another. Between them, a cylindrical opening permitted the insertion of a sealed glass vial containing the sample.

Due to the planar form of the sensor, its field of view is 180 degrees but with reduced sensitivity towards the sides (with a Lambertian response, according to the manufacturer, where the sensitivity is proportional to the cosine of the angle from the axis of the sensor). To ensure accurate color measurement, the samples were placed close to the sensor at approximately 5 mm, and their size was big enough to cover most of the field of view.

2.5.4. Data Acquisition

The prototype was programmed to provide RGB coordinates as the output. As compared to a regular spectrophotometer, our sensor can provide three simultaneous values in each measurement that can be used to characterize the color of the sample (single measurement) and to analyze the kinetics of the changes undergone by the sample (continuous measurement). The theoretical range for each of the three channels in RGB coordinates spans from 0 to 255 (8 bits), but under non-ideal illumination conditions (color temperature of the light source, surface reflection, or light intensity), it is usually quite narrower. The integration time of the sensor can be set from 2.4 ms to 700 ms to adjust for different light conditions or measurement requirements. We used the default integration time of 2.4 ms, reading the color every 0.1 s for the kinetics measurements.

3. Results and Discussion

3.1. Light Source

To establish whether a transmittance or reflectance approach was more appropriate for each of the setups according to the sample holders and sensing films, we compared the output of the RGB sensor using either the integrated LED light (reflectance mode) or the external LED (transmittance mode). We found that the reflectivity of the glass sides in the glass-made sample holder built for phosgene detection (Figure 2a), together with that of the glass substrate containing the sensing film for the detection of phosgene, resulted in the light emitted by the integrated LED being affected and the color measurements being inaccurate. Other authors have found similar issues when building low-cost spectrophotometers using flatbed scanners or similar devices [14,18]. Using an external LED oriented towards the sample opposite to the RGB sensor (i.e., transmittance mode) eliminated this problem, hence this setup was used with this sample holder in all the experiments regarding phosgene detection. In the other sample holder with glass vials containing PDMS-based films, we did not find strong differences between the two light sources. Although the glass of the vials could have provoked some light reflection, the round shape and the black PLA enclosure probably minimized it. In any case, the results were slightly better using the integrated LED in the reflectance mode, and therefore it was chosen for all the experiments involving biogenic amine sensing.

3.2. Sensing

3.2.1. Phosgene Detection

Upon exposure to phosgene vapors, Harrison's reagent embedded into the screen-printed TiO₂ films turned from colorless with a slight bluish tint due to the TiO₂ particles to an intense orange–yellow coloration (see Figure 3). This change was irreversible and depended on the concentration of phosgene. The chemical reaction pathway of Harrison's reagent and phosgene is well documented and can be found elsewhere [25,30].

As detected by the RGB sensor, the exposure to the 50 ppm phosgene vapors produced an increase in the R and G coordinates and a decrease in the B coordinate, matching the composite color observed in the films (Figure 4). The R coordinate increased following the same kinetics that were obtained previously using a laboratory spectrophotometer

and measuring the absorbance change at 464 nm [25], which corresponded to a perceived orange–yellow complementary color by the subtraction of the absorbed wavelengths. The G coordinate also increased but reached saturation much faster and did not seem to correlate well with the phosgene concentration. The B coordinate decreased with an inverse shape with respect to that of the R coordinate, but it eventually reached a value of zero, limiting its usability for the quantification of phosgene in short-term measurements or concentrations below the ppm range.

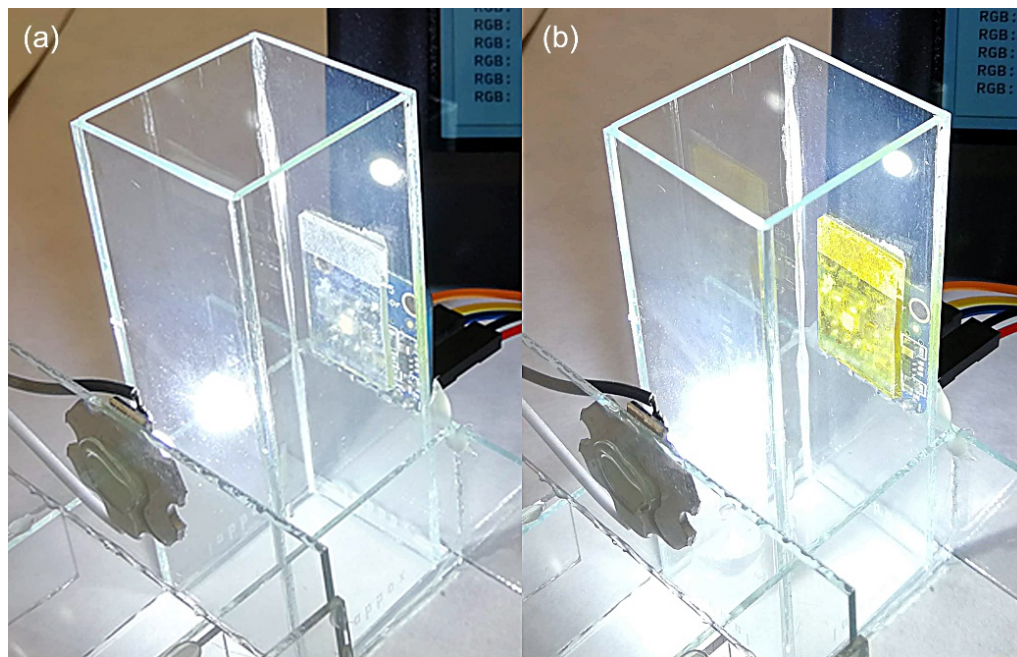


Figure 3. Screen-printed TiO₂ films containing Harrison’s reagent. (a) Initial status in air. (b) After exposure to phosgene vapors.

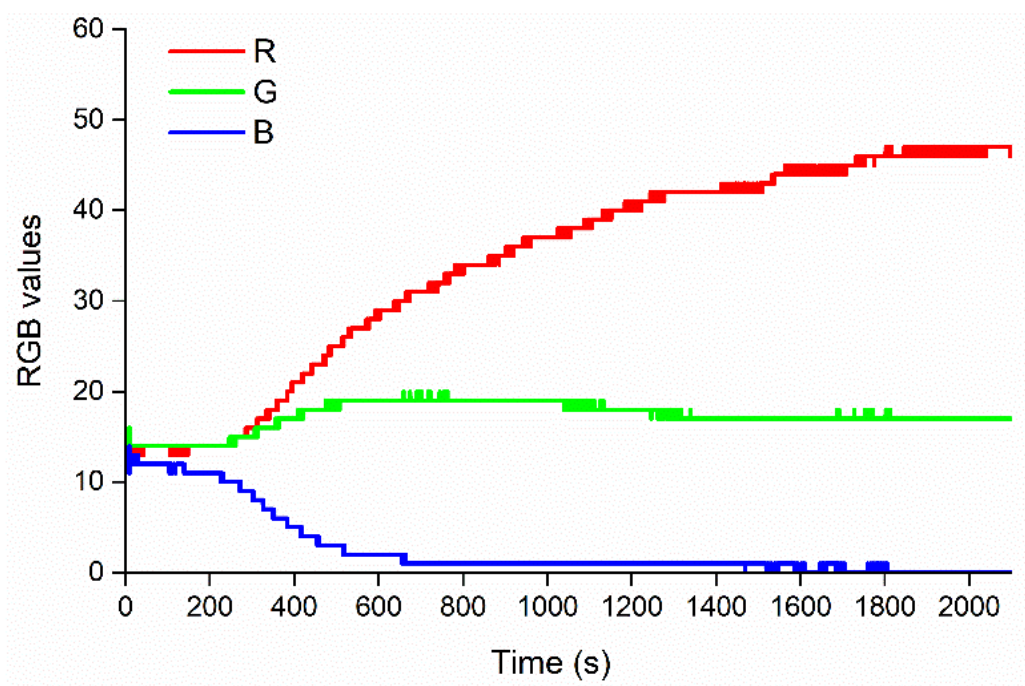


Figure 4. RGB kinetics of the exposure of Harrison’s reagent embedded into a screen-printed TiO₂ film to 50 ppm phosgene vapors.

The concentration dependence of the response was measured by analyzing the slope of the initial stage of the exposure (Figure 5a). The R coordinate of the RGB sensor was chosen for this purpose because it provided the best results among the three coordinates in terms of its range of usability and the correlation with the phosgene concentration. In addition, its behavior was similar to a spectrophotometer monitoring Harrison's reagent at its peak absorbance wavelength (464 nm), and this allowed for the comparison between the two methods. As expected, the response was faster the higher the phosgene concentration was, although the saturation limit was reached in all cases. Due to this, and to minimize the generation of highly toxic phosgene vapors, particularly when exposed to higher concentrations, the kinetics measurements were stopped before the saturation was reached and were limited to the initial portion of the response. Alternative analyses of the response in terms of the difference (R-B) or ratio (R/B) were considered to take advantage of dual-wavelength spectrophotometry [31], but they did not provide relevant results, which was probably due to the B coordinate reaching zero before the exposure was complete.

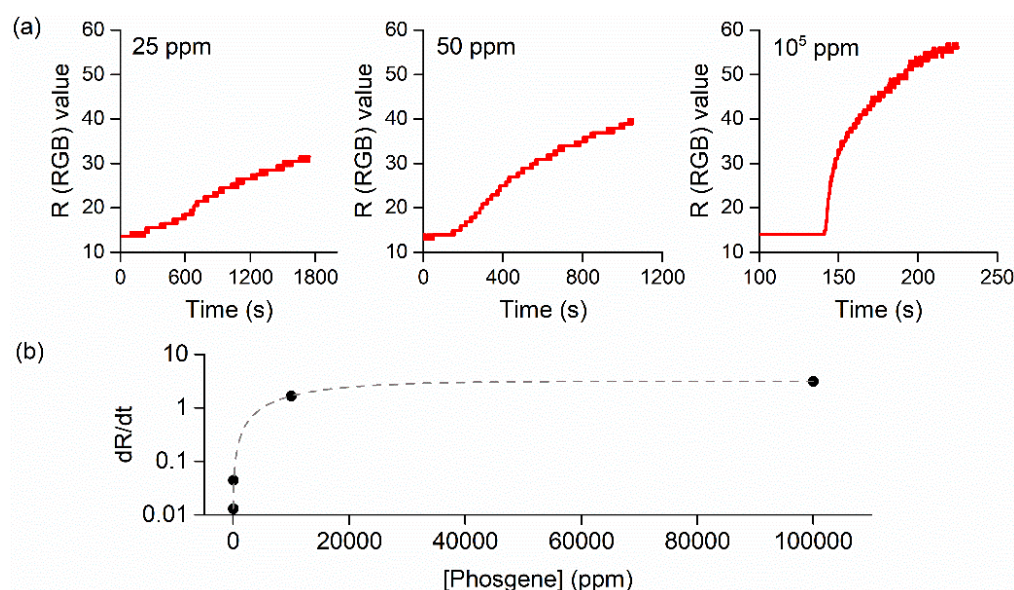


Figure 5. (a) Red coordinate's kinetics for the exposure of Harrison's reagent embedded into a screen-printed TiO₂ film to 25, 50, and 10⁵ ppm phosgene. (b) Calibration curve of the red coordinate's response rate as a function of the phosgene concentration. Symbols stand for experimental data. The dashed line corresponds to the exponential fit (see text for details).

To further characterize the response of the sensor, we performed a simple calibration using the R coordinate's variations as a function of the response time (t). For short and moderate times, the evolution of the signal can be defined as $S = M \cdot t$, where $M = dR/dt$. The response rates for each phosgene concentration (c) were fitted to an exponential curve $y = A + B \times \exp(C \times c)$ with coefficients $A = 3.14$, $B = -3.13$, and $C = -7.55 \times 10^{-5}$ ($R^2 = 0.99985$, $\chi^2 = 2.86706 \times 10^{-4}$). Figure 5b shows the resulting fit. Although more data at low concentrations would improve the calibration, we extracted the limit of detection (LOD) through the usual conventional signal-to-noise (S/N) ratio of 3. The LOD, calculated in the low-concentration regime for moderate exposure times, was found to be 0.5 ppm, which was below the immediately dangerous to life or health limit established at 2 ppm. A more exhaustive calibration for the colorimetric response in a lower concentration range was described in a previous work [25], which dealt with concentrations as low as 26 ppb, proving the ability of the device to detect concentrations even below the threshold limit value, which was set at 0.1 ppm. Even though the saturation limit of the sensor was equivalent for all the concentrations, the initial slope of the signal proved to be a robust indicator of the phosgene concentration. The aforementioned calibration using the slope of

the signal integrated the absorption, diffusion, and reaction of phosgene involved in the response of the sensor, reflecting its overall kinetics behavior.

3.2.2. Biogenic Amines Detection

To test the reversibility of the films and the ability of the prototype to monitor cycles of exposure and recovery, we used methylamine instead of the naturally generated biogenic amines. The slow release of biogenic amines during the bacterial decomposition of fish and their low vapor pressures did not allow for the concatenation of exposure–recovery cycles in a reasonable amount of time. Figure 6 shows the RGB color evolution of a pre-protonated PCN-224/PDMS film during a sequence of cycles of exposure to an atmosphere saturated in methylamine and the recovery through protonation with TFA vapors. As can be seen, the film experienced a decrease in the G coordinate and an increase in the R and B coordinates upon exposure to methylamine. Visually, the color of the films turned from green to reddish brown. All three cycles of exposure to methylamine reached the same RGB coordinates, which suggested the possible reusability of the films and confirmed the stability of the baseline of the RGB sensor. On the other hand, the protonation cycles with TFA led to an increase in the G coordinate and a decrease in the R and B coordinates, producing a green color in the films. In this case, the changes were increasing among consecutive cycles. This was not observable to the naked eye given that the films were of a similar green color, but the RGB analysis indicated that the protonation was not complete in the first cycles. We attributed this to the specific conditions established for these experiments. To be able to concatenate cycles of exposure to alternate vapors while measuring the color of the films, we could not allow the TFA to saturate the atmosphere during an appropriate amount of time. This probably led to a partial protonation during each of the cycles that did not reach the less-accessible molecules inside the film until the last cycles. In any case, the results provided by the prototype indicated that the films were usable from the first cycle due to the resolution of the RGB sensor and the intense color change of the PCN-224.

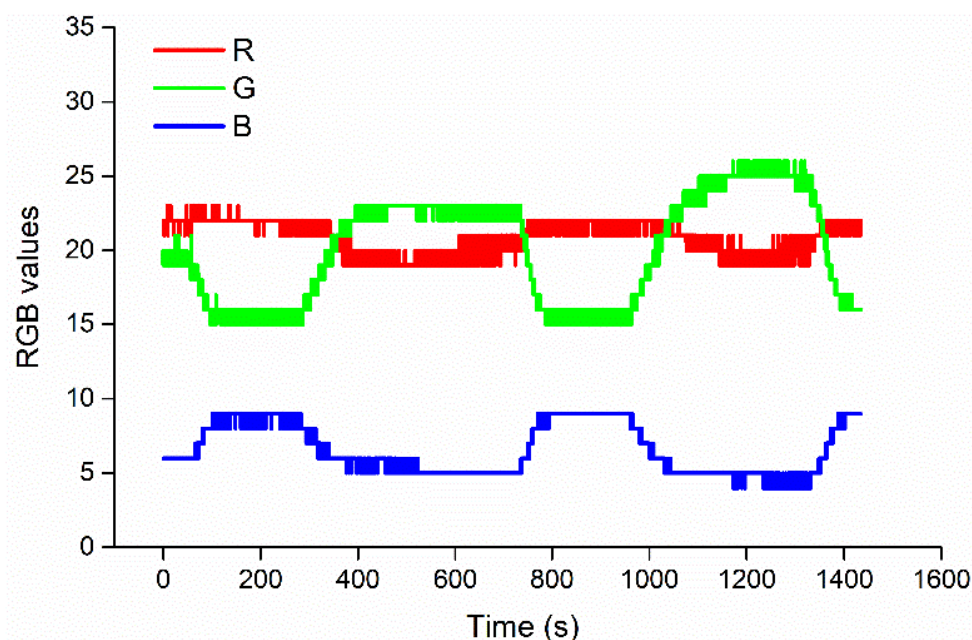


Figure 6. RGB kinetics of a PCN-224/PDMS film exposed to alternate cycles of methylamine and TFA.

The exposure of the PDMS/PCN-224 films to the biogenic amines generated from fish decomposition produced a color change from the initial (post-protonation) green to reddish brown after six days (Figure 7). These colors were indistinguishable from those in the methylamine experiments. The change, observable from the outside of the vial without breaking the seal of the vials, was gradual and with slight differences between fish species.

While the films exposed to the decomposition products from Atlantic salmon and Red mullet were reddish brown at the end of the experiment, those exposed to decomposed European anchovy remained partially green.

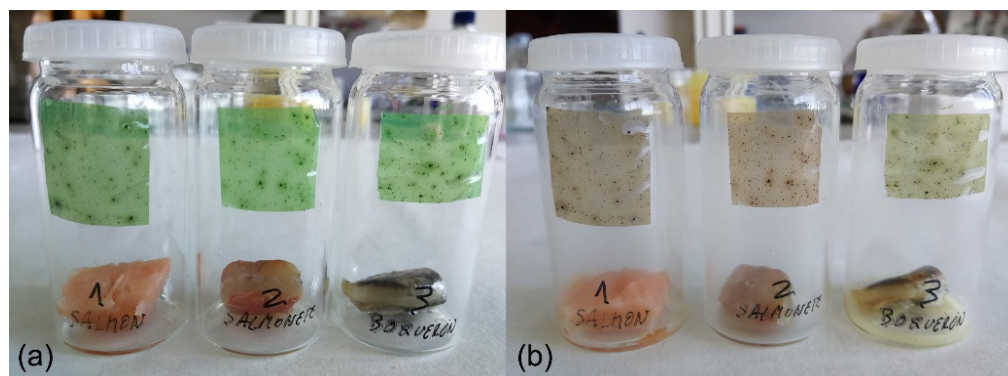


Figure 7. Sealed glass vials containing PCN-224/PDMS films and fish left to decompose. Left to right in both panels: Atlantic salmon (*Salmo salar*), Red mullet (*Mullus barbatus*), and European anchovy (*Engraulis encrasicolus*). (a) Initial status with fresh fish. (b) After six days of natural decomposition of fish at room temperature.

Detailed monitoring of the color changes experienced by the films during the natural decomposition of the fish samples was conducted using the RGB sensor in a custom 3D-printed sample holder, which permitted the measurement of the RGB coordinates using either the internal LED of the sensor or an external LED source without interference from ambient light. Although both illumination sources yielded similar results in terms of their tendencies and overall color identification, the measurements performed with the internal LED showed wider color ranges that improved the separation between data points, making it the preferred illumination method for this setup. To avoid breaking the seal of the vials and interrupting the accumulation of decomposition compounds in their internal atmospheres, the illumination and color measurement of the films were conducted from the outside of the vials. As can be seen in Figure 8, the evolution of the RGB coordinates followed the same tendency in all cases, with the R coordinate increasing, the G coordinate decreasing, and the B coordinate remaining stable or decreasing slightly, depending on the fish species. This was a clear translation of the observed color into the RGB color space, meaning the evolution from green to reddish brown, and was similar to the results obtained from the exposure to methylamine, especially regarding the G and R coordinates, which were responsible for most of the color of these sensing films. The B coordinate did not follow the same tendency among the fish species and, hence, no comparison could be made with the methylamine exposure. In any case, the low values in the B coordinate indicated a low presence of blue in the overall color of the films and did not provide much information in the analysis.

The differences between the species were evident in the analysis of the RGB coordinates. We focused on the results using the internal LED as light source, although these were comparable to those using the external light source. While the spoiled Atlantic salmon and Red mullet swiftly induced an increase in the R coordinate and a decrease in the G coordinate after 1–2 days, in the case of European anchovy this was not evident until day five. A plausible explanation for this is that the differences in the tissue composition according to the fish species affected the composition and amount of the compounds produced during the decomposition. Assuming this, the spoilage of European anchovy led to the emission of less biogenic amines than the other two species, which delayed the appearing of the reddish-brown color in our films. In any case, a detailed analysis of the composition of the fish and their decomposition products would be necessary to fully develop this hypothesis.

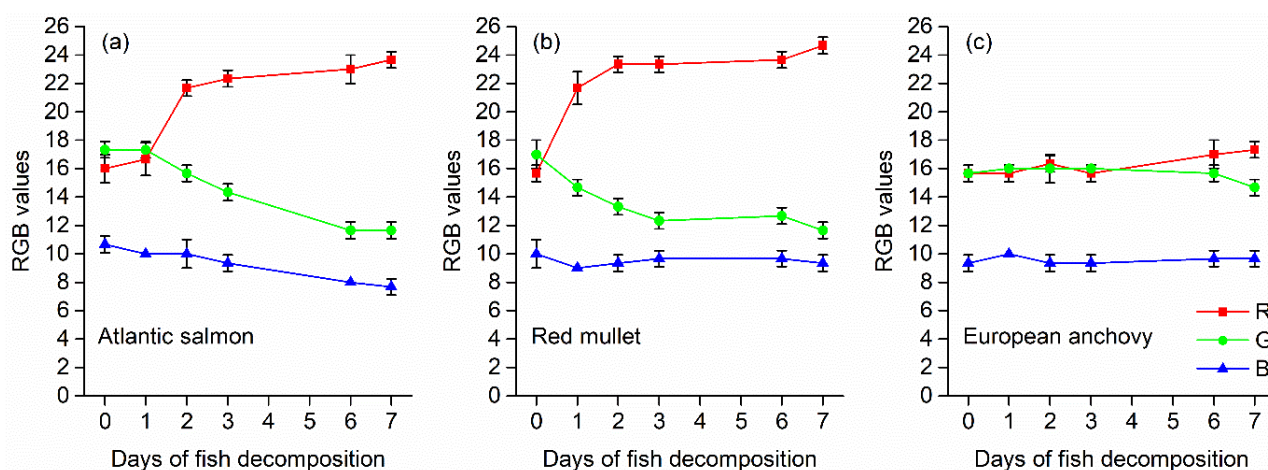


Figure 8. Color evolution (RGB coordinates) of PCN-224/PDMS films over six days of exposure to fish left to decompose. Left to right: (a) Atlantic salmon, (b) Red mullet, (c) European anchovy.

3.3. Comparison with Other Devices

To provide some insight about the main characteristics of low-cost colorimetric detectors to date, a comparison of our system to a selection of similar devices found in the literature is provided in Table 1. In all cases, the cost of the devices remained below EUR/USD 100, although some of the prices reported might need to be corrected to current markets. Among them, our device was one of the cheapest and was only more expensive than those reported by Swanson et al. [32] and Li et al. [33]. The most expensive was the one reported by Christodouleas et al. [14], although it is worth noting that they took advantage of off-the-shelf devices and had a high sample throughput. The sensors found in all the devices were effectively coupled to light sources, and none of them used ambient light to avoid illumination fluctuations. In this sense, the monochromatic LED ($\lambda = 642$ nm) used in Swanson et al. [32] limited its use to samples with a peak absorption near the LED emission wavelength. Ellerbee et al. [1], although they used a single photodetector that was unable to detect color, took advantage of a tricolor LED, whose color could be selected prior to the measurement. All the other devices, including ours, used sensors that were able to detect the color of the sample. As can be expected, the output after the measurement depended on the chosen detection system and could reflect either the color of the sample (e.g., RGB values) or just a transmitted or reflected intensity. In some cases [14], the output was in an image format and needed to be post-processed with imaging software to extract the information. Although this does not pose an important difficulty, it prevents the visualization of results in real-time.

Table 1. Main characteristics of a selection of low-cost colorimetric detectors.

Device	Cost	Sensor	Light Source	Output	Post-Processing	Programming
This study	~25 €	RGB	White LED	RGB values	No	Yes (Python)
Ellerbee et al. [1]	~\$50	Photodetector	Tricolor LED	Transmittance	No	No
Christodouleas et al. [14]	\$90/ unspecified ^(a)	CCD/CMOS image sensors	White LED	RGB-resolved absorbance	Yes	No
Swanson et al. [32]	~\$20 ^(b)	Photodiode	Monochromatic LED	Transmittance	No	Yes (C)
Li et al. [33]	~\$20	Color sensor (unspecified)	LED (unspecified)	Reflected light intensity	No	Yes (C)

^(a) Two devices were used, namely a flatbed scanner and a smartphone. The price of the latter was not specified, but was probably above USD 100 when the study was conducted. ^(b) Estimated by the authors for large-scale production.

Finally, some of these devices needed to be programmed after being built, and the ease-of-use of a device can be affected by this. However, this also offers the possibility of modifying the acquisition parameters and can expand the usability of the detection system to a wider range of situations. The device presented in this study runs on a short and simple Python script provided by the sensor manufacturer that allows for the modification of several parameters to fine-tune the measurements.

4. Conclusions

The prototype developed in this study could replace expensive equipment when the required application requires measuring the color change of any colorimetric device. With its small footprint alongside its low power consumption and the ability to run on a 5 V battery, our prototype is also highly portable, adding to its versatility. The combination of this device with gas-sensing colorimetric films such as those used in this study resulted in a complete and useful gas detection system that could be adapted for use in numerous applications.

Author Contributions: Conceptualization, J.M.P. and J.R.; methodology, J.R., F.G.M. and A.P.V.; software, J.R.; validation, J.M.P. and J.R.; formal analysis, J.R.; investigation, J.R., F.G.M. and A.P.V.; resources, J.M.P. and T.L.-C.; data curation, J.R.; writing—original draft preparation, J.R.; writing—review and editing, J.R. and J.M.P.; visualization, J.R.; supervision, J.M.P. and T.L.-C.; project administration, J.M.P. and T.L.-C.; funding acquisition, J.M.P. and T.L.-C. All authors have read and agreed to the published version of the manuscript.

Funding: This research was funded by the Spanish AEI/MCIN/10.13039/501100011033 within the NextGenerationEU/PRTR funds through the projects PCI2020-112241 (M-ERA.NET 2019 project 7106, SALMOS) and PID2019-110430 GB-C22 (ADLIGHT). ERDF (80%) and Andalusian CTEICU/JA in the framework of the Operative Programme FEDER Andalucía 2014–2020 through projects P20_01258 (objective 01) and UPO-1381028 (objective 1.2.3.) also contributed to the present research.

Institutional Review Board Statement: Not applicable.

Informed Consent Statement: Not applicable.

Data Availability Statement: The data presented in this study are available in the article.

Conflicts of Interest: The authors declare no conflict of interest.

References

1. Ellerbee, A.K.; Phillips, S.T.; Siegel, A.C.; Mirica, K.A.; Martinez, A.W.; Striehl, P.; Jain, N.; Prentiss, M.; Whitesides, G.M. Quantifying colorimetric assays in paper-based microfluidic devices by measuring the transmission of light through paper. *Anal. Chem.* **2009**, *81*, 8447–8452. [[CrossRef](#)] [[PubMed](#)]
2. Sia, S.K.; Linder, V.; Parviz, B.A.; Siegel, A.; Whitesides, G.M. An Integrated Approach to a Portable and Low-Cost Immunoassay for Resource-Poor Settings. *Angew. Chem.-Int. Ed.* **2004**, *43*, 498–502. [[CrossRef](#)] [[PubMed](#)]
3. Han, Y.D.; Chun, H.J.; Yoon, H.C. The transformation of common office supplies into a low-cost optical biosensing platform. *Biosens. Bioelectron.* **2014**, *59*, 259–268. [[CrossRef](#)]
4. Albert, D.R.; Todt, M.A.; Davis, H.F. A low-cost quantitative absorption spectrophotometer. *J. Chem. Educ.* **2012**, *89*, 1432–1435. [[CrossRef](#)]
5. Quagliano, J.M.; Marks, C.A. Demystifying spectroscopy with secondary students: Designing and using a custom-built spectrometer. *J. Chem. Educ.* **2013**, *90*, 1409–1410. [[CrossRef](#)]
6. Anzalone, G.C.; Glover, A.G.; Pearce, J.M. Open-source colorimeter. *Sensors* **2013**, *13*, 5338–5346. [[CrossRef](#)]
7. Asheim, J.; Kvittingen, E.V.; Kvittingen, L.; Verley, R. A simple, small-scale lego colorimeter with a light-emitting diode (LED) used as detector. *J. Chem. Educ.* **2014**, *91*, 1037–1039. [[CrossRef](#)]
8. Rohit; Kanwar, L.; Rao, K.K. Development of a low-cost portable colorimeter for the estimation of fluoride in drinking water. *Sens. Actuators B Chem.* **2010**, *149*, 245–251. [[CrossRef](#)]
9. Sumriddetchkajorn, S.; Chaitavon, K.; Intaravanne, Y. Mobile-platform based colorimeter for monitoring chlorine concentration in water. *Sens. Actuators B Chem.* **2014**, *191*, 561–566. [[CrossRef](#)]
10. Wei, Q.; Nagi, R.; Sadeghi, K.; Feng, S.; Yan, E.; Ki, S.J.; Caire, R.; Tseng, D.; Ozcan, A. Detection and spatial mapping of mercury contamination in water samples using a smart-phone. *ACS Nano* **2014**, *8*, 1121–1129. [[CrossRef](#)]
11. Cohen, A.R.; Seidl-Friedman, J. HemoCue® system for hemoglobin measurement. Evaluation in anemic and nonanemic children. *Am. J. Clin. Pathol.* **1988**, *90*, 302–305. [[CrossRef](#)] [[PubMed](#)]

12. Mieczkowska, E.; Koncki, R.; Tymecki, L. Hemoglobin determination with paired emitter detector diode. *Anal. Bioanal. Chem.* **2011**, *399*, 3293–3297. [[CrossRef](#)] [[PubMed](#)]
13. Okamura, K.; Kimoto, H.; Noguchi, T.; Hatta, M.; Kawakami, H.; Suzue, T. Colorimetric pH measurement for seawater samples using a three light-emitting diodes detector and a calibration method for temperature dependence. *Anal. Sci.* **2014**, *30*, 1135–1141. [[CrossRef](#)] [[PubMed](#)]
14. Christodouleas, D.C.; Nemiroski, A.; Kumar, A.A.; Whitesides, G.M. Broadly Available Imaging Devices Enable High-Quality Low-Cost Photometry. *Anal. Chem.* **2015**, *87*, 9170–9178. [[CrossRef](#)]
15. Knagge, K.; Rafferty, D. Construction and Evaluation of a LEGO Spectrophotometer for Student Use. *Chem. Educ.* **2002**, *7*, 371–375. [[CrossRef](#)]
16. Abbaspour, A.; Khajehzadeh, A.; Ghaffarinejad, A. A simple and cost-effective method, as an appropriate alternative for visible spectrophotometry: Development of a dopamine biosensor. *Analyst* **2009**, *134*, 1692–1698. [[CrossRef](#)] [[PubMed](#)]
17. Vashist, S.K.; van Oordt, T.; Schneider, E.M.; Zengerle, R.; von Stetten, F.; Luong, J.H.T. A smartphone-based colorimetric reader for bioanalytical applications using the screen-based bottom illumination provided by gadgets. *Biosens. Bioelectron.* **2015**, *67*, 248–255. [[CrossRef](#)]
18. Filippini, D.; Svensson, S.P.S.; Lundström, I. Computer screen as a programmable light source for visible absorption characterization of (bio)chemical assays. *Chem. Commun.* **2003**, 240–241. [[CrossRef](#)]
19. de Oliveira, H.J.S.; de Almeida, P.L.; Sampaio, B.A.; Fernandes, J.P.A.; Pessoa-Neto, O.D.; de Lima, E.A.; de Almeida, L.F. A handheld smartphone-controlled spectrophotometer based on hue to wavelength conversion for molecular absorption and emission measurements. *Sens. Actuators B Chem.* **2017**, *238*, 1084–1091. [[CrossRef](#)]
20. Benavides, M.; Mailier, J.; Hantson, A.L.; Muñoz, G.; Vargas, A.; Van Impe, J.; Wouwer, A. Vande Design and test of a low-cost RGB sensor for online measurement of microalgae concentration within a photo-bioreactor. *Sensors* **2015**, *15*, 4766–4780. [[CrossRef](#)]
21. Seelye, M.; Sen Gupta, G.; Bailey, D.; Seelye, J. Low cost colour sensors for monitoring plant growth in a laboratory. In Proceedings of the 2011 IEEE International Instrumentation and Measurement Technology, Hangzhou, China, 10–12 May 2011; pp. 972–977. [[CrossRef](#)]
22. Salmerón, J.F.; Gómez-Robledo, L.; Carvajal, M.Á.; Huertas, R.; Moyano, M.J.; Gordillo, B.; Palma, A.J.; Heredia, F.J.; Melgosa, M. Measuring the colour of virgin olive oils in a new colour scale using a low-cost portable electronic device. *J. Food Eng.* **2012**, *111*, 247–254. [[CrossRef](#)]
23. De La Torre, C.; Muñiz, R.; Pérez, M.A. A new, low-cost, on-line RGB colorimeter for wine industry based on optical fibers. In Proceedings of the 19th IMEKO World Congress, Lisbon, Portugal, 6–11 September 2009; Volume 4, pp. 2353–2357.
24. Ariono, M.R.E.; Budiman, F.; Silalahi, D.K. Design of Banana Ripeness Classification Device Based on Alcohol Level and Color Using a Hybrid Adaptive Neuro-Fuzzy Inference System Method BT. In Proceedings of the 1st International Conference on Electronics, Biomedical Engineering, and Health Informatics, Surabaya, Indonesia, 8–9 October 2020; Lecture Notes in Electrical, Engineering, Triwiyanto, Nugroho, H.A., Rizal, A., Caesarendra, W., Eds.; Springer: Singapore, 2021; pp. 107–117.
25. Vargas, A.P.; Gámez, F.; Roales, J.; Lopes-Costa, T.; Pedrosa, J.M. An Optical Dosimeter for the Selective Detection of Gaseous Phosgene with Ultralow Detection Limit. *ACS Sens.* **2018**, *3*, 1627–1631. [[CrossRef](#)] [[PubMed](#)]
26. Sousaraei, A.; Queirós, C.; Moscoso, F.G.; Silva, A.M.G.; Lopes-Costa, T.; Pedrosa, J.M.; Cunha-Silva, L.; Cabanillas-Gonzalez, J. Reversible Protonation of Porphyrinic Metal-Organic Frameworks Embedded in Nanoporous Polydimethylsiloxane for Colorimetric Sensing. *Adv. Mater. Interfaces* **2021**, *8*, 2001759. [[CrossRef](#)]
27. Feng, D.; Chung, W.C.; Wei, Z.; Gu, Z.Y.; Jiang, H.L.; Chen, Y.P.; Darendbourg, D.J.; Zhou, H.C. Construction of ultrastable porphyrin Zr metal-organic frameworks through linker elimination. *J. Am. Chem. Soc.* **2013**, *135*, 17105–17110. [[CrossRef](#)]
28. Moscoso, F.G.; Almeida, J.; Sousaraei, A.; Lopes-Costa, T.; Silva, A.M.G.; Cabanillas-Gonzalez, J.; Cunha-Silva, L.; Pedrosa, J.M. Luminescent MOF crystals embedded in PMMA/PDMS transparent films as effective NO₂ gas sensors. *Mol. Syst. Des. Eng.* **2020**, *5*, 1048–1056. [[CrossRef](#)]
29. Roales, J.; Pedrosa, J.M.J.M.; Guillén, M.G.M.G.; Lopes-Costa, T.; Pinto, S.M.A.S.M.A.; Calvete, M.J.F.M.J.F.; Pereira, M.M.M.M. Optical detection of amine vapors using ZnTriad porphyrin thin films. *Sens. Actuators B Chem.* **2015**, *210*, 28–35. [[CrossRef](#)]
30. Ryan, T.A.; Ryan, C.; Seddon, E.A.; Seddon, K.R. *Phosgene and Related Carbonyl Halides*; Elsevier: Amsterdam, The Netherlands, 1996; ISBN 9780080538808.
31. Cowles, J.C. Theory of Dual-Wavelength Spectrophotometry for Turbid Samples. *J. Opt. Soc. Am.* **1965**, *55*, 690–692. [[CrossRef](#)]
32. Swanson, C.; Lee, S.; Aranyosi, A.J.; Tien, B.; Chan, C.; Wong, M.; Lowe, J.; Jain, S.; Ghaffari, R. Rapid light transmittance measurements in paper-based microfluidic devices. *Sens. Bio-Sens. Res.* **2015**, *5*, 55–61. [[CrossRef](#)]
33. Li, B.; Fu, L.; Zhang, W.; Feng, W.; Chen, L. Portable paper-based device for quantitative colorimetric assays relying on light reflectance principle. *Electrophoresis* **2014**, *35*, 1152–1159. [[CrossRef](#)]

Disclaimer/Publisher’s Note: The statements, opinions and data contained in all publications are solely those of the individual author(s) and contributor(s) and not of MDPI and/or the editor(s). MDPI and/or the editor(s) disclaim responsibility for any injury to people or property resulting from any ideas, methods, instructions or products referred to in the content.